

Aleksander Lisiecki, Zbigniew Rokita, Dariusz Ginalski, Andrzej Kośny,
Wojciech Pakieła

Laser Welding of Ferritic Stainless Steel 1.4509 Used in the Manufacturing of Catalyst Housings and Diesel Particulate Filters

Abstract: The article discusses the results of tests as well as quality assessments of test joints made of tubes having a nominal thickness of 1.5 mm, a rectangular cross-section and a width of 140 mm and a length of 240 mm, made of ferritic stainless steel grade 1.4509 with the addition of microagents and used in the production of catalyst housings and diesel particulate filters. Test joints were made using a prototype line equipped with a TruDisk 2002 disk laser (TRUMPF) at a ROCH production plant in Tarnowskie Góry. The tests involved the preparation of an experimental batch of tubes. The tubes used in the tests were subjected to various procedures, i.e. only to laser welding (5 specimens), to the rolling of the weld surface after laser welding (5 specimens) and to the additional heat treatment of the joint area after welding (5 specimens). Most of the test welded joints represented high quality level B and were characterised by tensile strength not lower than that of the base material as well as by high plasticity confirmed in the Erichsen cupping test. However, slight undercuts of the weld root revealed in the tests indicated the risk of the partial lack of penetration or the formation of excessive undercuts in the production process. The foregoing necessitates the strict application of the welding procedure and, in particular, the ensuring of the high precision of laser beam positioning and accuracy when preparing sheet edges before welding.

Keywords: laser welding, stainless ferritic steel, disk laser, microstructure and properties

DOI: [10.17729/ebis.2022.3/1](https://doi.org/10.17729/ebis.2022.3/1)

Introduction

The housing of particulate filters and catalysts constitutes an integral and commonly used element of exhaust systems in today's combustion engine vehicles. The housing, made of

stainless steel, e.g. 1.4509, 1.4510 or 1.4512 (in accordance with PN-EN 10088), containing additions of niobium and titanium, is a crucial catalyst component. Because of difficult operating conditions including high temperature (up

Dr hab. inż. Aleksander Lisiecki, Professor at the Silesian University of Technology, Department of Welding, Gliwice; mgr inż. Zbigniew Rokita – ROCH Sp. z o. o.; Dariusz Ginalski – ROCH Sp. z o. o.; mgr inż. Andrzej Kośny – ROCH Sp. z o. o.; dr inż. Wojciech Pakieła – Department of Engineering Materials and Biomaterial

to 800°C), thermal fatigue and stresses as well as thermal shocks, such as contact with cold water or slush (often containing road salt) and exposure to highly corrosive and aggressive exhaust as well as in order to ensure necessary tightness during vehicle operation, the housing must be characterised by high corrosion resistance and mechanical (also fatigue) strength. The unsealing of the filter or catalyst housing is classified as a failure requiring the repair or the replacement of the entire component. The multi-annual production practice indicates that the area characterised by the highest risk of unsealing and perforation is the longitudinal weld (of the housing) and the area adjacent to it. In addition, other phenomena accompanying the attachment of catalysts include the formation of cracks or the excessive deformation (bend) of the welded joint.

The attachment of the catalyst involves putting the catalyst insert inside the housing along with an insulating mat. The forcing of the insert (using a dedicated calibrator) inside the housing is followed by clamping the housing around the insert. The next stage involves the welding of inlet and outlet hoppers. An alternative finishing method consists in the closing of the housing and forming the inlet and outlet hoppers through spinning (Fig. 1). The afore-said method makes it possible to eliminate the welding of subsequent elements (i.e. the formation of welded joints being the most susceptible to perforation and unsealing). However, the method, being less popular than the welding of the joints, yet increasingly often preferred by customers, requires the improvement of strength-related parameters of the welded joint.

In addition, the clamping and spinning processes are usually accompanied by the formation of defects and the scrapping of the catalyst insert (made of brittle ceramics and being the most expensive element of the exhaust system). The most typical reason for the above-presented situation is the improper quality of the housing related to the overly low strength of the

welded joint (leading to its bending or rupture and, consequently, to the cracking of the catalyst insert). This, in turn, necessitates increasingly high quality requirements concerning the filter housing, aimed to reduce the number of scrapped inserts.

The above-named issue inspired tests aimed to develop and implement a technology enabling the laser welding of housings of catalysts and particulate filters as well as ensuring the obtainment of the required quality and functional properties of joints.



Fig. 1. Catalyst housing made of a tube (through spinning) (a) and the ceramic catalyst insert (b)

Test

The objective of the work was to assess the quality of test joints made of tubes (circular blanks) 1.4509 having a nominal thickness of 1.5 mm, a rectangular cross-section and a width of 140 mm and a length of 240 mm. The tubes were made of ferritic stainless steel grade 1.4509 with the addition of microagents (Tables 1 and 2, Fig. 5). The welding process was performed using a disk laser (without the filler metal). The process involved the melting of interface edges and areas adjacent to the butting faces of tubes (Fig. 2). The tests were performed using an experimental batch of 15 tubes (in the form of circular blanks) provided by the ROCH company seated in Tarnowskie Góry. The specimens were welded on a pilot line equipped with a TruDisk 2002 disk laser (TRUMPF) and located in a production plant in Tarnowskie Góry (Figures 3 and 4). The tests involved joints directly after welding (designated as VAI1-VAI5) as well as joints subjected



Fig. 2. Test tubes made of 1.5 mm thick stainless steel 1.4509 in the ROCH company, prepared for joint quality-related tests and assessment; laser welded test tubes not subjected to any other treatment (five on the left), laser welded test tubes with the weld subjected to rolling (five in the middle) and laser welded test tubes with the welded joint subjected to additional heat treatment (five on the right)



Fig. 3. Window of the panel for controlling welding process parameters (a) and windows of the laser operation control panel (b)

to additional procedures such as the rolling of the weld (designated as VAI11-VAI15) and heat treatment (designated as VAII11-VAII15). The purpose of the above-named procedures was to reduce welding stresses and improve plastic properties of the material in the joint area (weld, HAZ) (Fig. 2).

Hardness and microhardness measurements were performed using a 401 MVD Vickers microhardness tester. Observations of the



Fig. 4. Prototype station for the heat treatment of tube fragments (designed and made at the ROCH company)

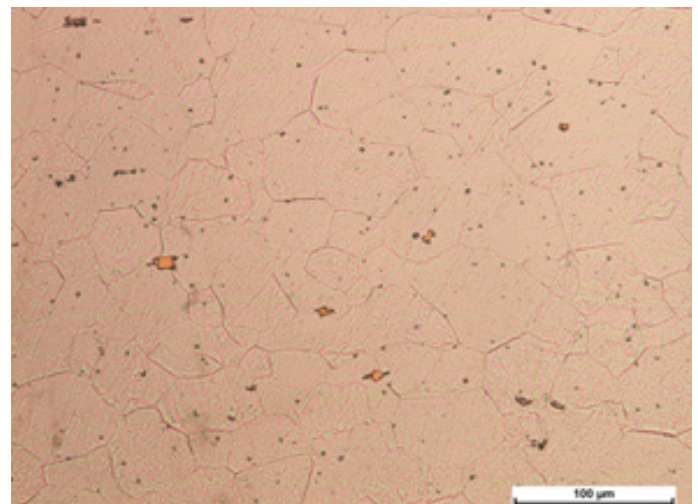
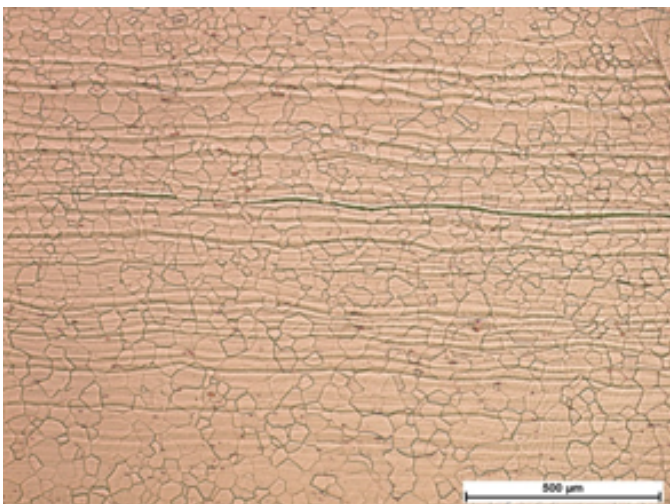


Fig. 5. Microstructure of the base material of 1.5 mm thick stainless steel 1.5409macrostructure

Table 1. Chemical composition of stainless steel 1.4509 (EN 10088-2)

Chemical composition; % by weight							
C	Mn	Si	P	S	Cr	Nb	Ti
0.03	1.0	1.0	0.04	0.015	17.5 – 18.5	0.3 – 1.0	0.1– 0.6

of the test joints were performed using an OLYMPUS SZX9 stereoscopic microscope and a magnification of up to 25 times. In turn, the microstructure of the test joints was observed and analysed using an ECLIPSE MA100 inverted microscope with a maximum image magnification of up to 1000 times.

The quality of the laser welded joints was assessed in accordance with the PN-EN ISO 5817 standard. The test joints subjected to visual tests are presented in Figures 6 through 8. Each test joint was sampled for three specimens used in metallographic tests, i.e. one sampled in the initial area (30 mm from the welding process starting point), one sampled at the half of the joint length and one sampled in the final area

Table 2. Mechanical properties of steel 1.4509 (EN 10088-2)

Tensile strength R_m , MPa	Yield point $R_{p0.2}$, MPa	Elongation at rupture A_{90} , %
430–630	230–250	18

(approximately 30 mm away from the edge of the tube). Representative macrostructures of the test joints are presented in Figures 9 through 11, whereas the images of microstructures are presented in Figures 12 through 14. The microstructure on the surface of the metallographic specimens was revealed through the process of electrolytic etching.

The microhardness measurements were performed using a test rig featuring a 401 MVD microindentation hardness tester (Wilson

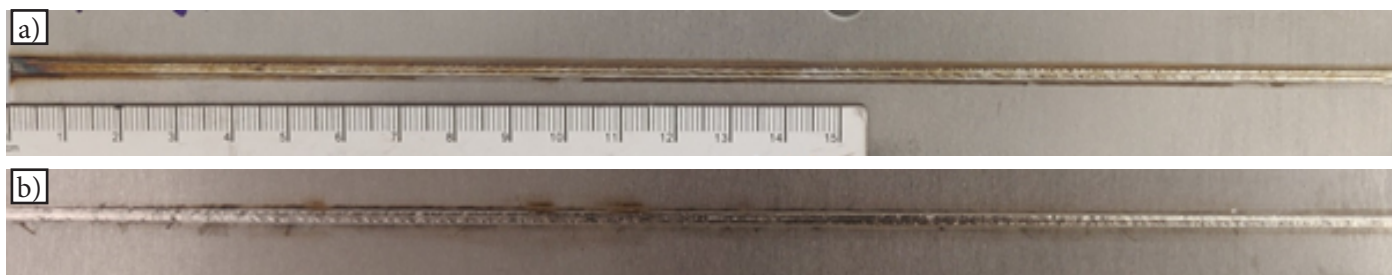


Fig. 6. Surface of the weld face (a) and of the weld root (b) of the butt welded joint (designated as AVI) made of 1.5 mm thick steel 1.4509 (tube), directly after laser welding

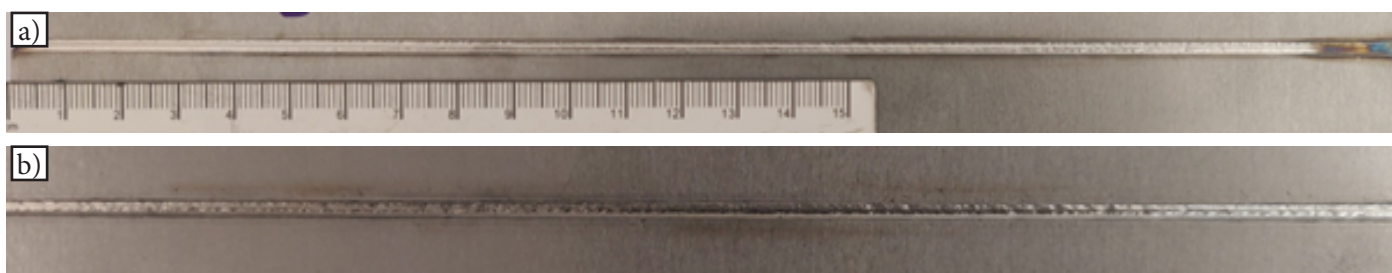


Fig. 7. Surface of the weld face (a) and of the weld root (b) of the butt welded joint (designated as AVI) made of 1.5 mm thick steel 1.4509 (tube) after the rolling of the weld

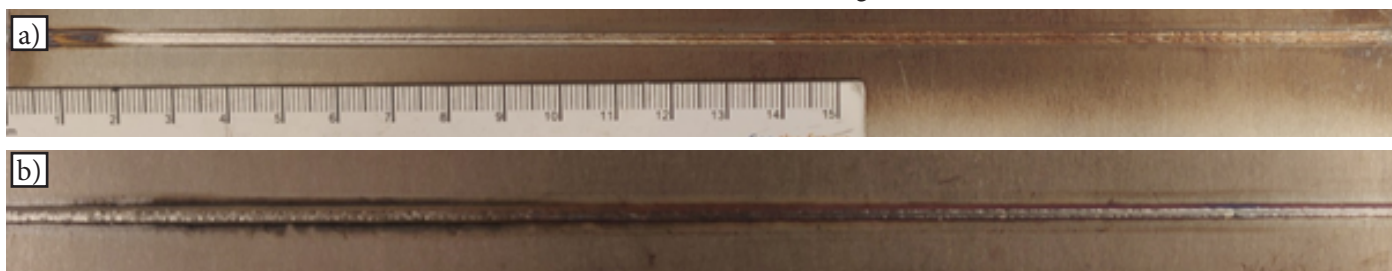


Fig. 8. Surface of the weld face (a) and of the weld root (b) of the butt welded joint (designated as AVI) made of 1.5 mm thick steel 1.4509 (tube) after the rolling of the weld and heat treatment

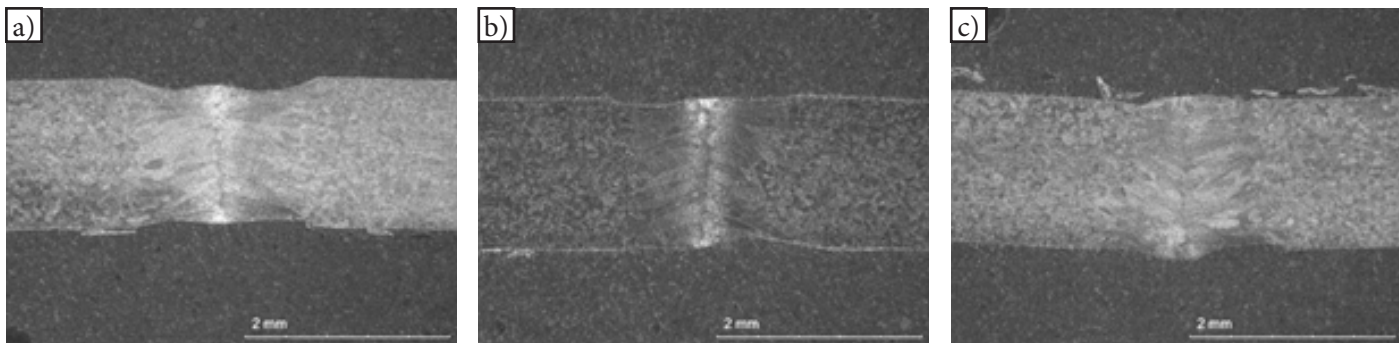


Fig. 9. Macrostructure of the longitudinal butt welded joint (designated as AVI) made of 1.5 mm thick steel 1.4509 (tube) directly after laser welding: a) initial area of the weld, b) central area of the weld and c) final area of the weld

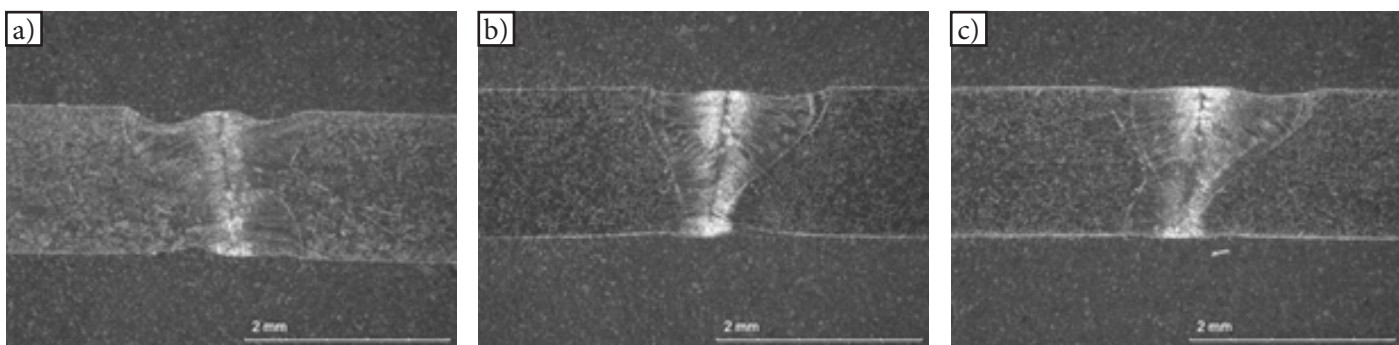


Fig. 10. Macrostructure of the longitudinal butt welded joint (designated as AVI) made of 1.5 mm thick steel 1.4509 (tube) after laser welding and the additional rolling of the weld surface: a) initial area of the weld, b) central area of the weld and c) final area of the weld

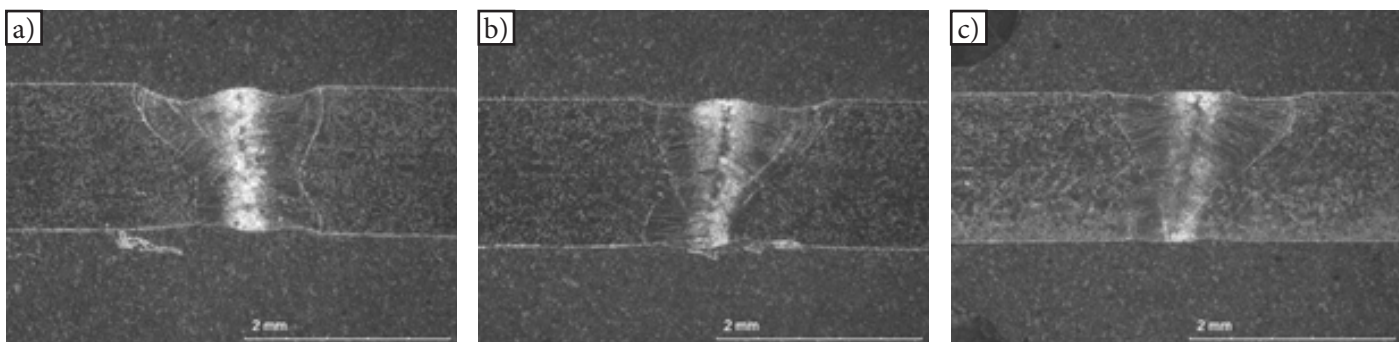


Fig. 11. Macrostructure of the longitudinal butt welded joint (designated as AVI) made of 1.5 mm thick steel 1.4509 (tube) after laser welding, the additional rolling of the weld surface and the heat treatment of the joint: a) initial area of the weld, b) central area of the weld and c) final area of the weld

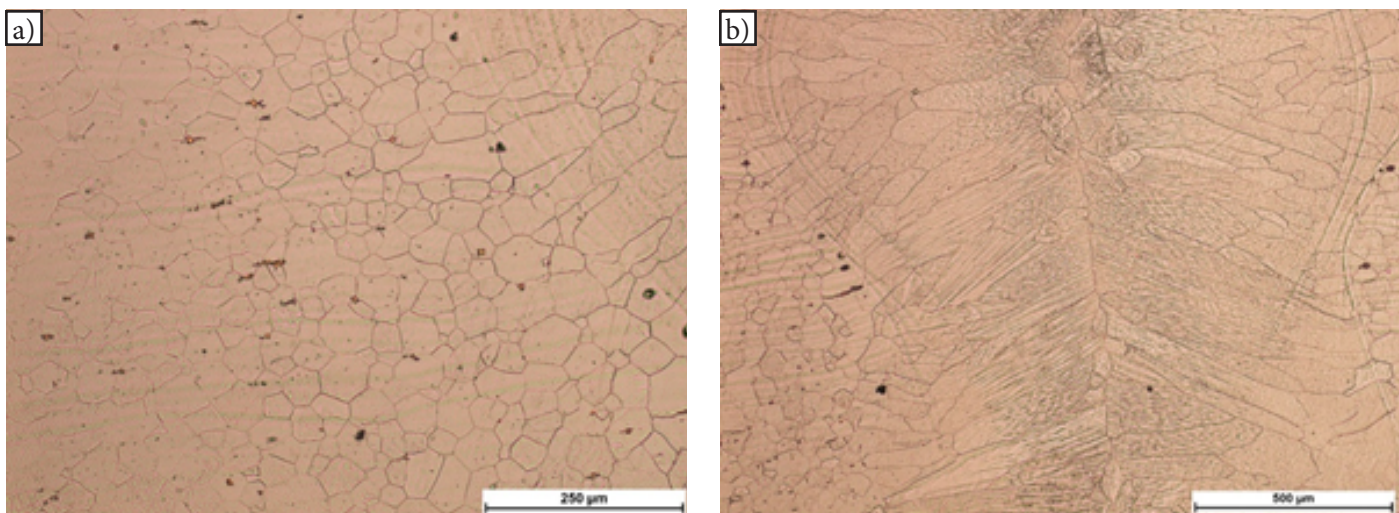


Fig. 12. Microstructure of the longitudinal butt welded joint (designated as AVI) made of 1.5 mm thick steel 1.4509 (tube) directly after laser welding: a) from the left: BM, HAZ, fusion line, weld and b) weld area

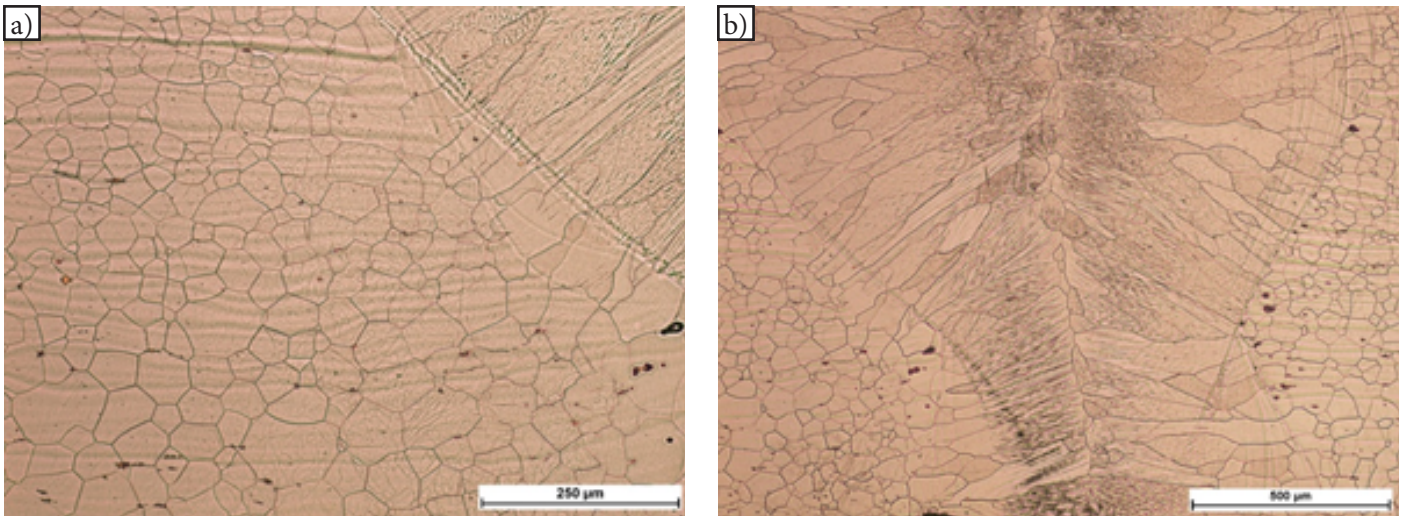


Fig. 13. Microstructure of the longitudinal butt welded joint (designated as AVI) made of 1.5 mm thick steel 1.4509 (tube) directly after laser welding and the additional rolling of the weld surface: a) from the left: BM, HAZ, fusion line, weld and b) weld area

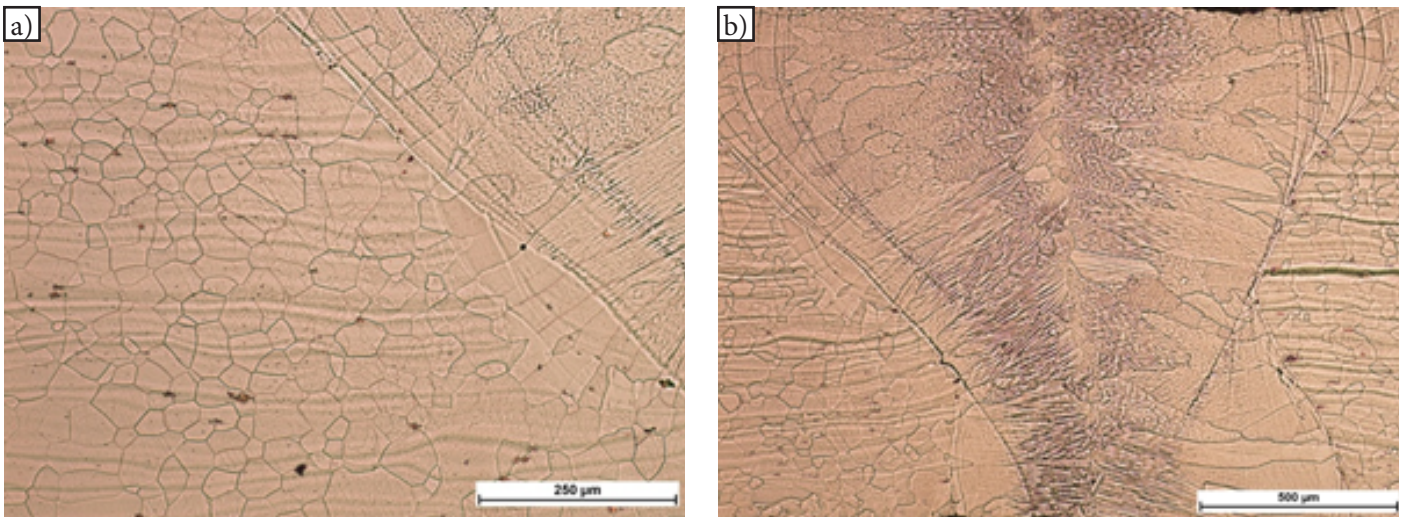


Fig. 14. Microstructure of the longitudinal butt welded joint (designated as AVI) made of 1.5 mm thick steel 1.4509 (tube) directly after laser welding, the additional rolling of the weld surface and the heat treatment of the joint: a) from the left: BM, HAZ, fusion line, weld and b) weld area

Wolpert), calibrated directly before the measurements. The measurements, involving the use of a diamond indenter load of 200g (HVo.2) and a load operating time of 10 s, were performed along the entire length of the specimen, with measurement points located every 0.5 mm. In relation to all the specimens, the measurements involved the base material, the

heat affected zone (HAZ) and the weld. The schematic diagram presenting the performance of the measurements is presented in Figure 15, whereas the measurement results are presented in Figure 16.

The tensile tests of the joints involved the use of a Z 100 testing machine (Zwick), enabling the obtainment of a maximum tensile

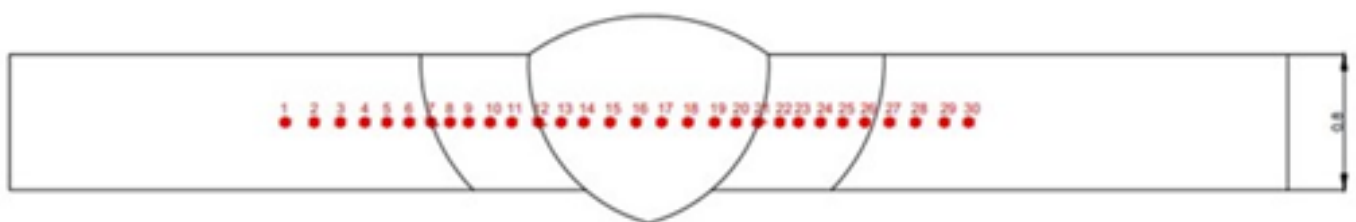


Fig. 15. Schematic diagram presenting hardness measurements in the cross-section of the test joints (test direction from left to right)

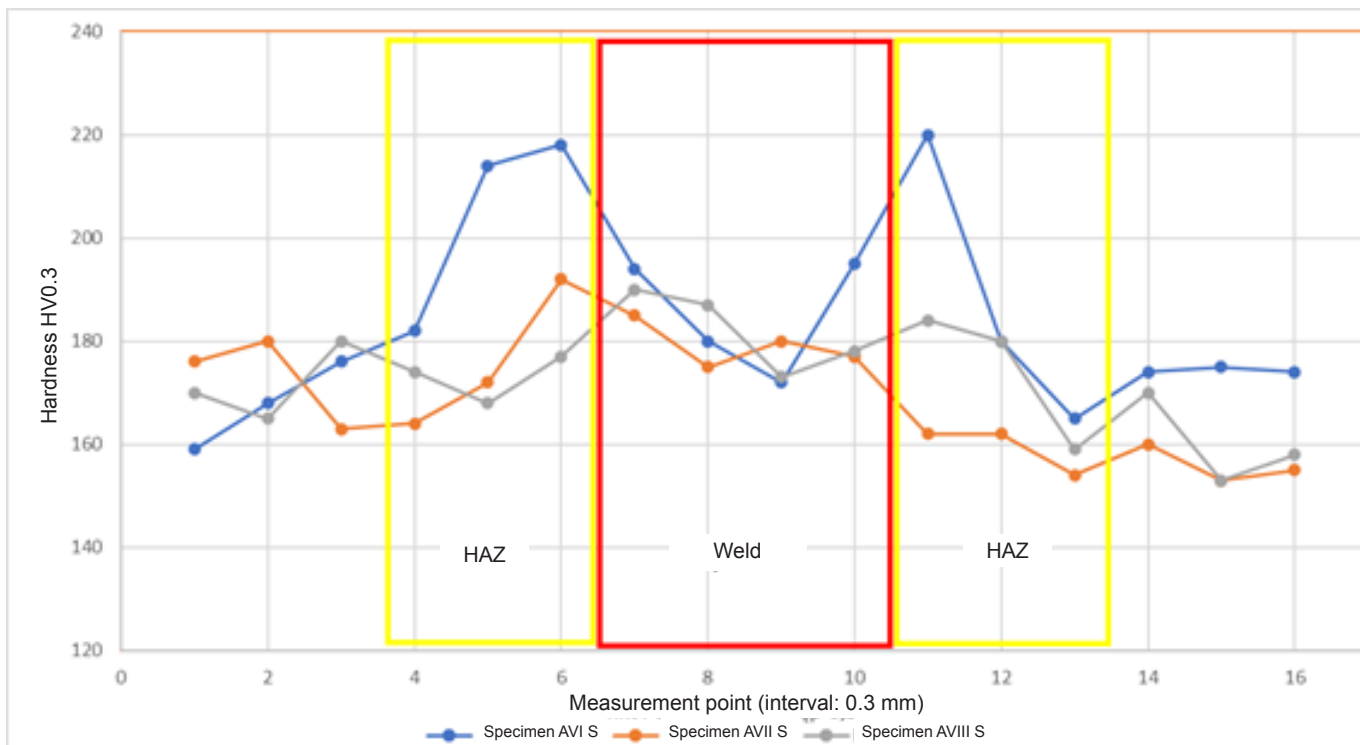


Fig. 16. Changes of microhardness in the cross-section of the test joints made of 1.5 mm thick stainless steel (tube) (designated as AVI – directly after laser welding, AVII – after laser welding and the rolling of the weld, AVIII – after laser welding, the rolling of the weld and additional heat treatment)

strength of 100 kN. The tests were performed in accordance with the procedure consistent with the DIN EN ISO 6892-1 standard. In turn, the specimens used in the mechanical tests were prepared in accordance with PN-EN ISO 4136 *Destructive tests on welds in metallic materials – Transverse tensile test*. Because of the fact that the test welded joints constituted the heterogeneous material, the only parameter determined in the tensile test was tensile strength.

The test rig and the tensile test itself are presented in Figure 17. In turn, the specimens after rupture are presented in Figure 18. The tensile test-related diagrams are presented in Figures 19 and 20. The specimens after the Erichsen cupping test are presented in Figure 21.

Analysis of results

The visual tests revealed that the width of the weld on the face side did not exceed 1.5 mm. In turn, on the root side, the weld was even narrower and amounted to 1.2 mm in relation to all the test joints. The width of the weld face and that of the weld root were uniform along the entire length of the test joints. The weld face surface was flat and even, with a clearly visible line in the weld axis, formed as a result of the solidification of the weld pool and related to a fast laser welding rate. It was also possible to observe the slightly incompletely filled groove. Because of the narrow width of the weld and the shallow depth of the incompletely filled groove, the performance of measurements was impossible during visual tests (VT). As regards the laser welding of butt joints without the filler metal,

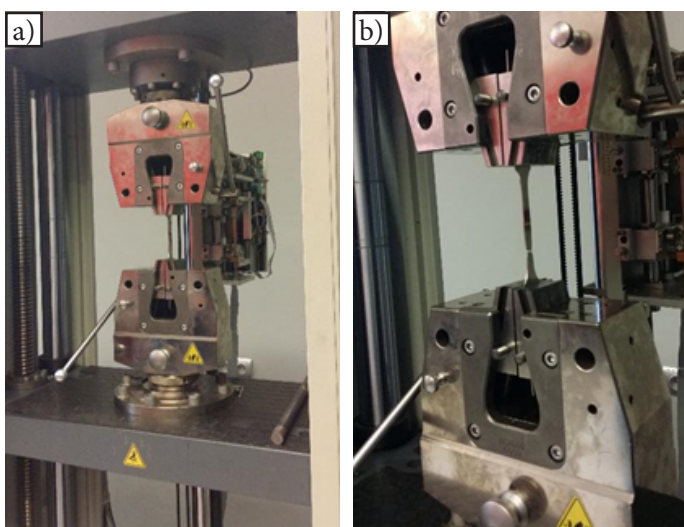


Fig. 17. Specimen in the clamps of the Z 100 testing machine (Zwick) (a) and the specimen ruptured in the static tensile test (b)



Fig. 18. Specimens used in the static tensile test, sampled from the laser welded test tubes made of 1.5 mm stainless steel 1.5409 (a) and the specimens after the static tensile test – rupture outside the weld (b)

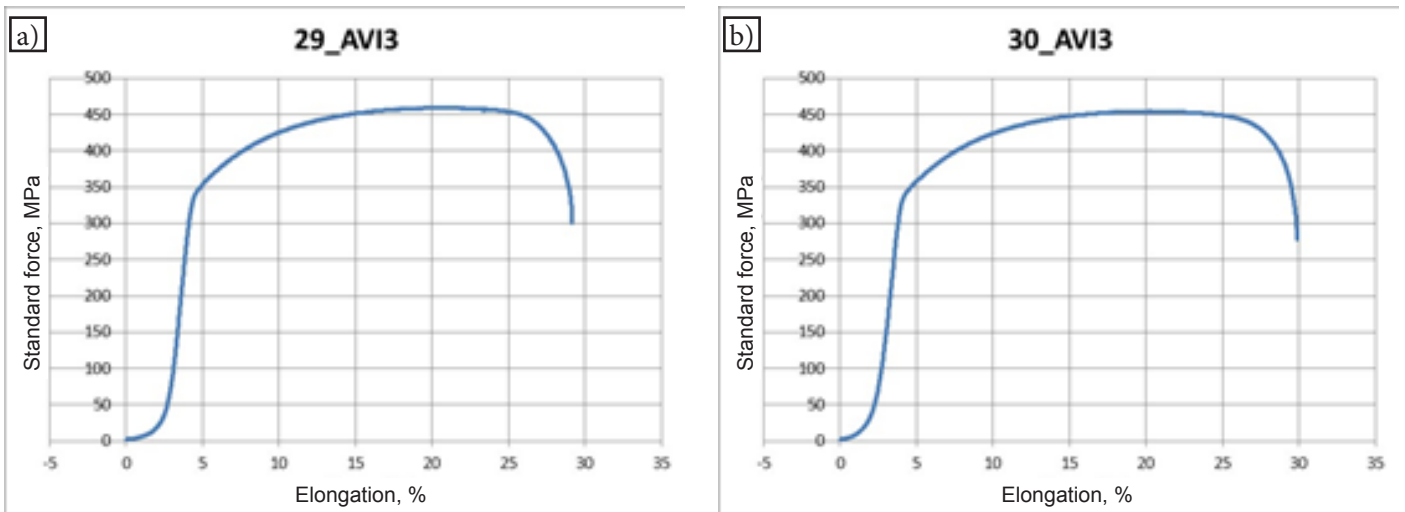


Fig. 19. Results of the static tensile test of the longitudinal test butt joint made of 1.5 mm thick stainless 1.4509 (tube); the test was performed directly after laser welding (tensile strength (rupture in BM) $R_m \sim 450$ MPa)

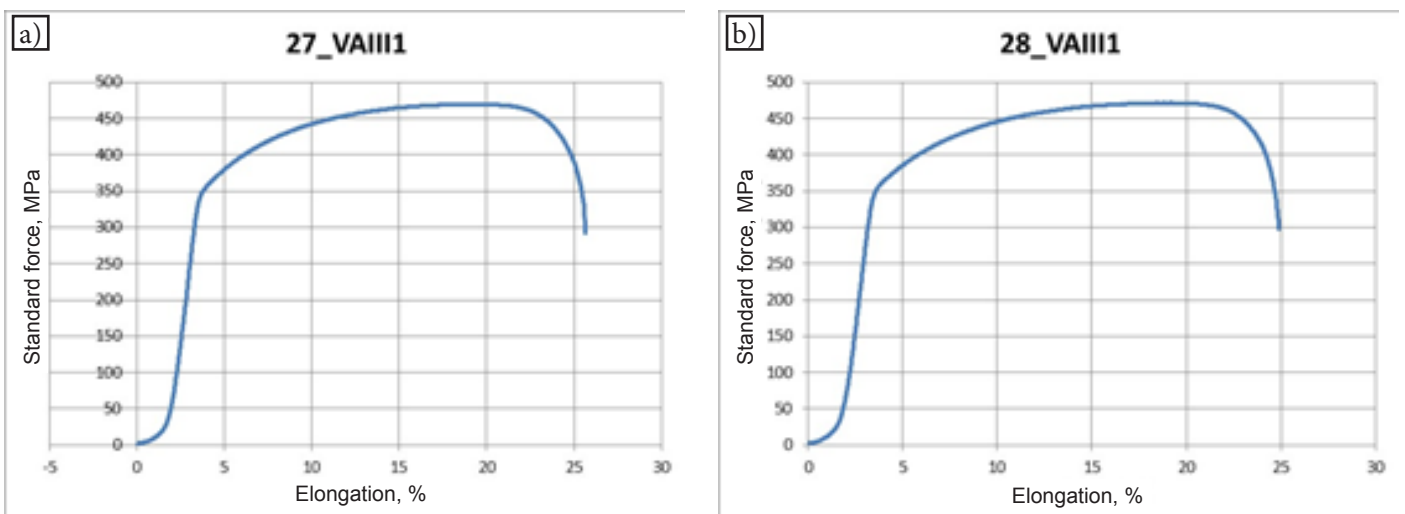


Fig. 20. Results of the static tensile test of the longitudinal test butt joint made of 1.5 mm thick stainless 1.4509 (tube); the test was performed after laser welding, the rolling of the weld and the heat treatment of the joint area (tensile strength (rupture in BM) $R_m > 450$ MPa)

the formation of the aforesaid incompletely filled groove is a natural phenomenon, resulting primarily from the presence of a narrow gap between the butting faces of the sheets subjected to welding. In addition, the incompletely filled groove is acceptable because of the ultimate application of the test joints, i.e. in the making of housings of catalysts and particulate filters of exhaust systems in combustion engine vehicles.

Criteria governing the acceptance of welded elements, specified by the end recipient, permit the slightly incompletely filled groove. The visual tests also revealed the presence of craters located both at the beginning and at the end of all of the test joints. The presence of craters at the welding process starting area was connected with a sharp increase in laser beam power and initially unstable thermal conditions. In turn, the craters at the end of the weld were formed as a result of a sudden laser beam shut-down and weld metal solidification conditions in this area. Although the phenomenon of crater formation is natural, it is at the same time unfavourable as the presence of craters increases the likelihood of crack formation during plastic working performed within the production process.

The visual tests also revealed the presence of discolouration on the weld face surface and in the areas along the face of the joints. In the joints subjected to heat treatment, the area containing discolouration was even wider (restricted within the range of approximately 10 mm to 15 mm on each side of the weld). The heat treatment-triggered oxidation was strictly present on the surface and should not adversely affect the mechanical properties of the joints.

The macroscopic tests and observations of the fusion line shape enabled the further assessment concerning the quality of the joints and the parametrisation of the welding imperfection

identified during the visual tests, i.e. the incompletely filled groove. Measurements involving the surface of the metallographic specimens sampled from various areas of the test joints (initial (initial area – I, central area – C and final area – F) revealed that the depth of the incompletely filled groove in the central area of the weld did not exceed 0.15 mm, i.e. the value acceptable in accordance with the adopted quality-related criteria. The measurements concerning the width of the weld on the surface of metallographic specimens revealed that the width of the weld face of the test joints was restricted within the range of approximately 1.1 mm to 1.5 mm. In turn, the weld root was significantly narrower, with its width being restricted within the range of approximately 0.5 mm to a maximum of 1.2 mm in relation to all of the test joints.

The method applied during the electrolytic etching of the metallographic specimens and the use of polarising filters of microscopic images made it possible to obtain the contrast of the individual areas of the joint and determine the width of the HAZ. The measurements revealed that the width of the zone characterised by structural changes was restricted within the range of approximately 0.4 mm to 0.6 mm. It was also possible to observe a narrow zone of grain growth in the area adjacent to the fusion line and a zone of grain refinement (in relation to the grain size observed in the base material).

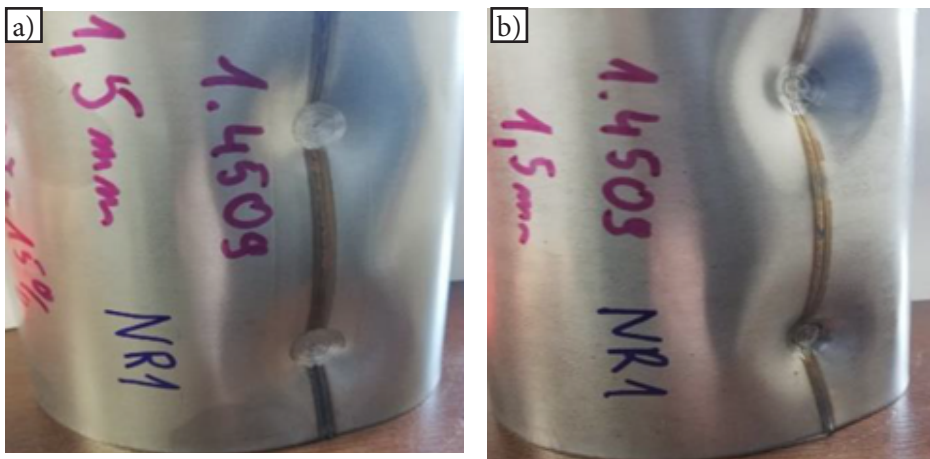


Fig. 21. Specimens after the Erichsen cupping test performed along the longitudinal butt joint of the tube: a) joint after the rolling of the weld (IE: 16.0 mm) and b) joint after the rolling of the weld and additional heat treatment (IE: 16.5 mm)

The macrostructural observations also made it possible to identify the direction of the build-up of columnar crystals in the weld area. It was noticed that, after nucleation in partially melted grains of the material subjected to welding, the crystals built up perpendicularly to the fusion line. In turn, the faces of the columnar crystals building up in opposite directions “met” in the weld axis. The aforesaid manner of weld pool solidification was responsible for the fact the columnar crystals were elongated and characterised by significantly larger cross-sections than those of the base material grains and HAZ grains. In turn, the central area of the weld also contained grains of various sizes and arrangement, formed at the final phase of weld solidification. The aforesaid area could be characterised by the segregation of alloying components, in particular impurities, inclusions and low-melting eutectics, which could adversely affect mechanical properties of joints.

The morphology of base material grains was typical of ferrite. However, at the same time, both the base material and the HAZ contained significant amounts of precipitates located primarily along the grain boundaries. In the microstructural images, the aforesaid precipitates were visible as fine golden particles of various (i.e. triangular, trapezoidal or polygonal) shapes. Because of the chemical composition of the steel and the mechanism of its hardening during production, the precipitates were probably highly dispersed carbides or carbonitrides. The weld areas did not contain precipitates of similar morphology. Observations of the weld microstructure performed at high magnification revealed the presence of single gas pores of small diameters (not longer than 80 μm) as well as the presence of inclusions both in the HAZ and in the base material. The diameter of the inclusions did not exceed 20 μm .

Cross-sectional microhardness measurements revealed that the hardness of the base material amounted to approximately 160 HV_{0.2}. In cases of the laser welded test joints made using

a linear energy of 50 J/mm the distribution of hardness in the cross-section of the welded joint revealed a significant increase in hardness in the HAZ and in the weld, restricted within the range of approximately 218 HV_{0.2} to 220 HV_{0.2}. In turn, the rolling of the welded joint area led to the favourable evening of the weld surface and of the joint edge, which could positively affect subsequent technological operations connected with the fabrication of the filter housing or the fixing of the catalyst insert. The hardness measurement results also revealed that the rolling of the joints was not followed by a clearly visible increase in average hardness values in the cross-section of the joints; recorded values were restricted within the range of 185 HV_{0.2} to 193 HV_{0.2}. Tests concerning the distribution of hardness in the cross-section of the joints subjected to heat treatment performed using adopted parameters revealed that the process did not translate into a significant decrease in hardness in the weld and in the HAZ. The average values of hardness in the cross-section of the joints subjected to heat treatment were restricted within the range of 185 HV_{0.2} to 190 HV_{0.2}.

All of the specimens ruptured outside the joint area, away from the weld. The test results revealed that the tensile strength of the base material was not lower than 450 MPa. The rupture of the specimens outside the joint area resulted from the hardening of the weld area and of the HAZ during the laser welding process.

The results of the Erichsen cupping tests revealed that the Erichsen value (drawability index) of the joints satisfied requirements concerning the base material of the sheets (IEm_{in} 12 mm). The foregoing implies that tubes made using the laser welding process and additional technological procedures can be subjected to further plastic working at the subsequent stages of catalyst production.

Summary

The above-presented test results revealed that most of the test joints represented quality level B,

yet slight weld root undercuts indicated the risk of the partial lack of penetration or excessive undercuts formed during the production process and related to the inadequate precision of laser beam positioning or lower accuracy of pre-weld sheet edge preparation. It is therefore necessary to strictly follow procedures concerned with material preparation, i.e., in particular, dimensional and shape-related accuracy, the precise preparation of sheet edges, the removal of impurities as well as the repeatable fixing and stiffening of circular blanks during the welding process.

The tests discussed in the article were performed within EU-funded project no. UDA-RPSL.01.02.00-24-00-00B8/19-00.

References

- [1] Li G.J., Liu X.L.: Literature review on research and development of automotive lightweight technology. *Mater. Sci. Technol.*, 2020, no. 28, pp. 47–61.
- [2] Ohjoo K., Lee K.Y., Kim G.S., Chin K.G.: New trends in advanced high strength steel developments for automotive application. *Mater. Sci. Forum*, 2010, no. 884, pp. 136–141.
- [3] Goss C., Marecki P., Muszyński T., Torzewski J.: Badania porównawcze połączeń spawanych ze stali wysoko wytrzymałych stosowanych na konstrukcje pojazdów specjalnych. *TTS Technika Transportu Szynowego*, 2015, vol. 22, no. 12, pp. 572–575.
- [4] Holzner A.: Spawanie wysokowytrzymałych drobnoziarnistych stali konstrukcyjnych metodą MAG drutami proszkowymi. *Biuletyn Instytutu Spawalnictwa*, 2011, no. 4, pp. 39–48.
- [5] Grajcar A.: Technologie łączenia wysokowytrzymałych blach stalowych dla motoryzacji. *Stal, Metale & Nowe Technologie*, 2016, 9–10, pp. 39–43.
- [6] Kumar N., Mukherjee M., Bandyopadhyay A.: Comparative study of pulsed Nd:YAG laser welding of AISI 304 and AISI 316 stainless steels. *Optics & Laser Technology*, 2017, no. 88, pp. 24–39.
- [7] Das A., Fritz R., Finut M., Masters I.: Blue laser welding of multi-layered AISI 316L stainless steel micro-foils. *Optics & Laser Technology*, 2020, no. 132, 106498.
- [8] Alhajhamoud M., et al.: Laser Welding of 316L Austenitic Stainless Steel in an Air and a Water Environment. *Materials*, 2022, no. 15, 2248.
- [9] Mokhtari M., Pommier P., Balcaen Y., Alexis J.: Laser Welding of AISI 316L Stainless Steel Produced by Additive Manufacturing or by Conventional Processes. *J. Manuf. Mater. Process.*, 2021, no. 5, pp. 136.
- [10] Lisiecki A., Kurc-Lisiecka A.: Automated laser welding of AISI 304 stainless steel by disk laser. *Arch. Metall. Mater.*, 2018, vol. 63, no. 4, pp. 1663–1672.
- [11] Landowski M., Świerczyńska A., Rogalski G., Fydrych D.: Autogenous Fiber Laser Welding of 316L Austenitic and 2304 Lean Duplex Stainless Steels. *Materials*, 2020, no. 13, pp. 2930.
- [12] Pańcikiewicz K., Świerczyńska A., Hućko P., Tumidajewicz M.: Laser Dissimilar Welding of AISI 430F and AISI 304 Stainless Steels. *Materials*, 2020, no. 13, pp. 4540.
- [13] Kurc-Lisiecka A., Lisiecki A., Juroszek W.: Spawanie laserowe złączy blach ze stali AISI 316. *STAL Metale & Nowe Technologie*, 2016, no. 11–12, pp. 40–44.
- [14] Kurc-Lisiecka A.: Spawanie laserowe złączy doczołowych z austenitycznej stali nierdzewnej AISI 304. *STAL Metale & Nowe Technologie*, 2018, no. 11–12, pp. 69–73.
- [15] Topolska S., Łabanowski J.: Effect of microstructure on impact toughness of duplex and superduplex stainless steels. *Journal of Achievements in Materials and Manufacturing Engineering*, 2009, no. 36, pp. 142–149.
- [16] Brytan Z., Vademecum stali nierdzewnej, *Stowarzyszenie Stali Nierdzewnej*, 2018.